Microwave Rotational Spectra of 2-Bromofurane and 3-Bromofurane and Bromine Nuclear Quadrupole Coupling Tensors

M. Stolze, D. Hübner, and D. H. Sutter

Abteilung für Chemische Physik im Institut für Physikalische Chemie der Christian-Albrechts-Universität zu Kiel

Z. Naturforsch. **36a**, 886–898 (1981); received June 4, 1981

The vibronic ground state rotational spectra are reported for the ^{79}Br- and ^{81}Br-species of 2-Bromofurane and 3-Bromofurane. Both μ_a and μ_b-type spectra were observed. The small inertia defects confirm that the equilibrium configurations are planar. From the nuclear quadrupole coupling tensors it may be concluded that π-contributions to the C-Br bonds are smaller than in the Halobenzenes.

Introduction

We started our investigation of the rotational spectra of the Bromofuranes because of our interest in substituent effects on the magnetic properties of small aromatic molecules. In the following we present the analysis of the pure rotational spectra of the Bromofuranes in their vibronic ground states. Such an analysis is the prerequisite for a subsequent rotational Zeeman effect study. The rotational constants and Bromine nuclear quadrupole coupling constants so obtained provide some information on the molecular structure and make it possible to judge the amount of double bond character present in the C-Br-bond.

Experimental and Data Analysis

2-Bromofurane and 3-Bromofurane were obtained from EGA-Chemie, Steinheim, West Germany. The pure compounds are colourless liquids with boiling points of 102 °C ($p = 744$ Torr) [1]) and 102.5 °C ($p = 745$ Torr) [1]) respectively. If stored at room temperature they slowly turn brownish due to oxidation products. They were used after a vacuum distillation without further purification.

The spectra were recorded with a standard Hughes-Wilson type [2]) microwave spectrometer with 33.3 kHz Stark-effect modulation and phase stabilized backward wave oscillators as radiation sources. With the two Bromine isotopes having natural abundancies of 50.5% (^{79}Br) and 49.5% (^{81}Br), a fairly strong Br-quadrupole hyperfine coupling, and with several low frequency vibrations present in the molecules, the spectra are dense and population distribution over many low energy states leaves comparatively little absorption intensity in the individual rotational transitions. In addition each spectrum actually consists of two, one arising from the interaction of the electric field vector of the incident microwave radiation with the a-component of the permanent molecular electric dipole moment and a second arising from its interaction with the b-component (c-axis perpendicular to the molecular plane).

From vector addition of the experimental electric dipole moments of Furane [3] and Bromobenzene [4] see Figure 1, the a-type spectra may be estimated to be stronger by a factor on the order of 20

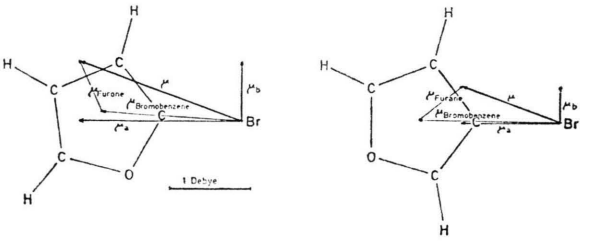

Fig. 1. Rotational transition selection rules depend on the nonzero components of the permanent electric dipole moment. In the case of the Bromofuranes $\mu_c = 0$ due to the planarity of the equilibrium structures. μ_a and μ_b may be estimated from the dipole moments of Furane [5] and Bromobenzene [6] even though the resulting absolute values are slightly different from those reported for the liquid phase [2]. With absorption intensities proportional to the square of the dipole moment component which acts as the lever to change the specific rotational state, the μ_a-type transitions are stronger by a factor of approximately 10(2-Bromofurane) to 20(3-Bromofurane) than the μ_b-type transitions.

Reprint requests to Prof. Dr. D. H. Sutter, Institut für Physikalische Chemie der Universität Kiel, Abteilung Chemische Physik, Olshausenstraße 40–60, D-2300 Kiel.

0340-4811 / 81 / 0800-0886 $ 01.00/0. — Please order a reprint rather than making your own copy.

Dieses Werk wurde im Jahr 2013 vom Verlag Zeitschrift für Naturforschung in Zusammenarbeit mit der Max-Planck-Gesellschaft zur Förderung der Wissenschaften e.V. digitalisiert und unter folgender Lizenz veröffentlicht: Creative Commons Namensnennung-Keine Bearbeitung 3.0 Deutschland Lizenz.

This work has been digitalized and published in 2013 by Verlag Zeitschrift für Naturforschung in cooperation with the Max Planck Society for the Advancement of Science under a Creative Commons Attribution-NoDerivs 3.0 Germany License.

Zum 01.01.2015 ist eine Anpassung der Lizenzbedingungen (Entfall der Creative Commons Lizenzbedingung „Keine Bearbeitung") beabsichtigt, um eine Nachnutzung auch im Rahmen zukünftiger wissenschaftlicher Nutzungsformen zu ermöglichen.

On 01.01.2015 it is planned to change the License Conditions (the removal of the Creative Commons License condition "no derivative works"). This is to allow reuse in the area of future scientific usage.

if compared to the b-type transitions. Thus the assignment of the spectra was accomplished in a two step procedure. First the a-type spectra were predicted from rotational constants calculated under the assumption of an undistorted Furane ring [5] and a C-Br distance of 1.85 Å taken from Bromobenzene [6]. Although this prediction proved rather crude, it was possible to assign the a-type transitions on the basis of their typical quadrupole hyperfine patterns (see Figs. 2 and 3) and from the selfconsistency of the corresponding least squares fit. We confirmed the assignment by microwave-microwave double resonance experiments [7] using the setup shown in Figure 4. From the fit of the rotational constants and quadrupole coupling constants to the observed a-type frequencies accurate B and C rotational constants and less accurate A rotational constants were obtained which could be used to reduce the uncertainties in the predicted frequencies of the weak b-type transitions. In the second step the b-type transitions were searched and assigned. Again we used the microwave-microwave double resonance technique to filter the weak μ_b-type transitions from the djungle of weak μ_a-type absorptions originating from molecules in high-J-states or from molecules in excited vibrational states. In these experiments we typically set the signal frequency on top of a well known a-type transition in the Ku-frequency band while the strong X-band pump radiation was slowly swept over the region where the corresponding μ_b-type transition was suspected to reside (see insert on Figure 4). Five μ_b-type transitions were identified unambiguously this way for each isotope, sufficient to derive accurate values for all rotational constants and molecular quadrupole coupling constants. The complete listings of observed frequencies are given in Tables 1 and 2 (2-Bromofuranes) and Tables 3 and 4 (3-Bromofuranes). The corresponding rotational constants and the elements of the Br-quadrupole coupling tensors are listed in Tables 5 and 6.

For the analysis of the data we used the standard rigid rotor Hamiltonian including the quadrupole

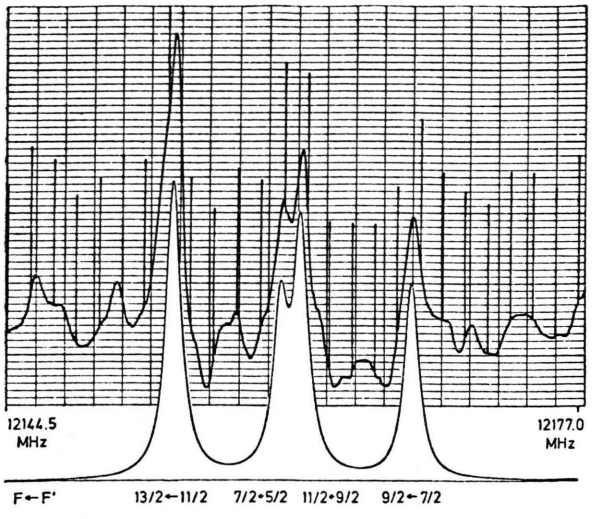

Fig. 2. Broad band scan (upper trace) and computer simulation (lower trace) covering the frequency range of the $5_{15} \leftarrow 4_{14}$ transition (μ_a-type) of 2-Bromofurane (^{79}Br). The wavy baseline is caused by weaker still unassigned transitions and by Stark-lobes. (Absorption in the off-phase of the 1.2 kV/cm square wave modulation is written upwards, absorption in the on-phase is written downwards by the phase sensitive detection scheme). The individual hyperfine satellites are marked by the F quantum numbers of the upper and lower state respectively.

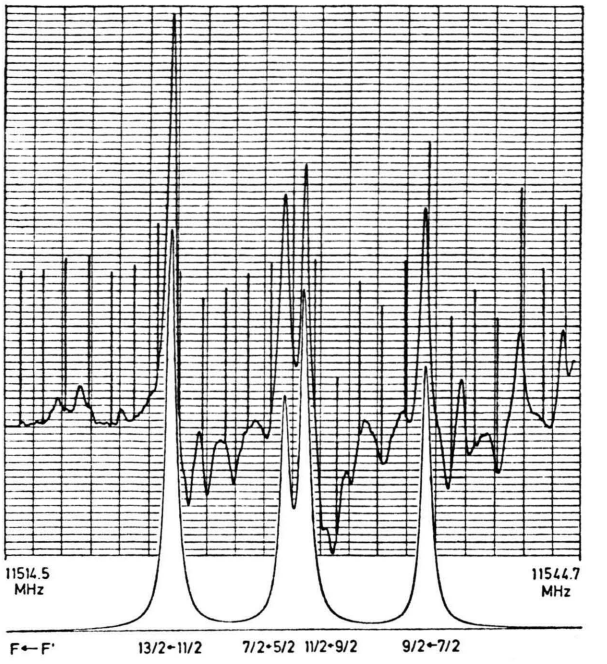

Fig. 3. Broad band scan and computer simulation covering the frequency range of the $5_{15} \leftarrow 4_{14}$ transition of 3-Bromofurane (^{79}Br) (compare Fig. 2 for the corresponding transition in 2-Bromofurane). Due to the smaller μ_b-component, the intensity of μ_b-type transitions would be weaker by a factor of about 20. Even though they could be identified and measured with high accuracy by use of the microwave-microwave double resonance spectrometer shown in Figure 4.

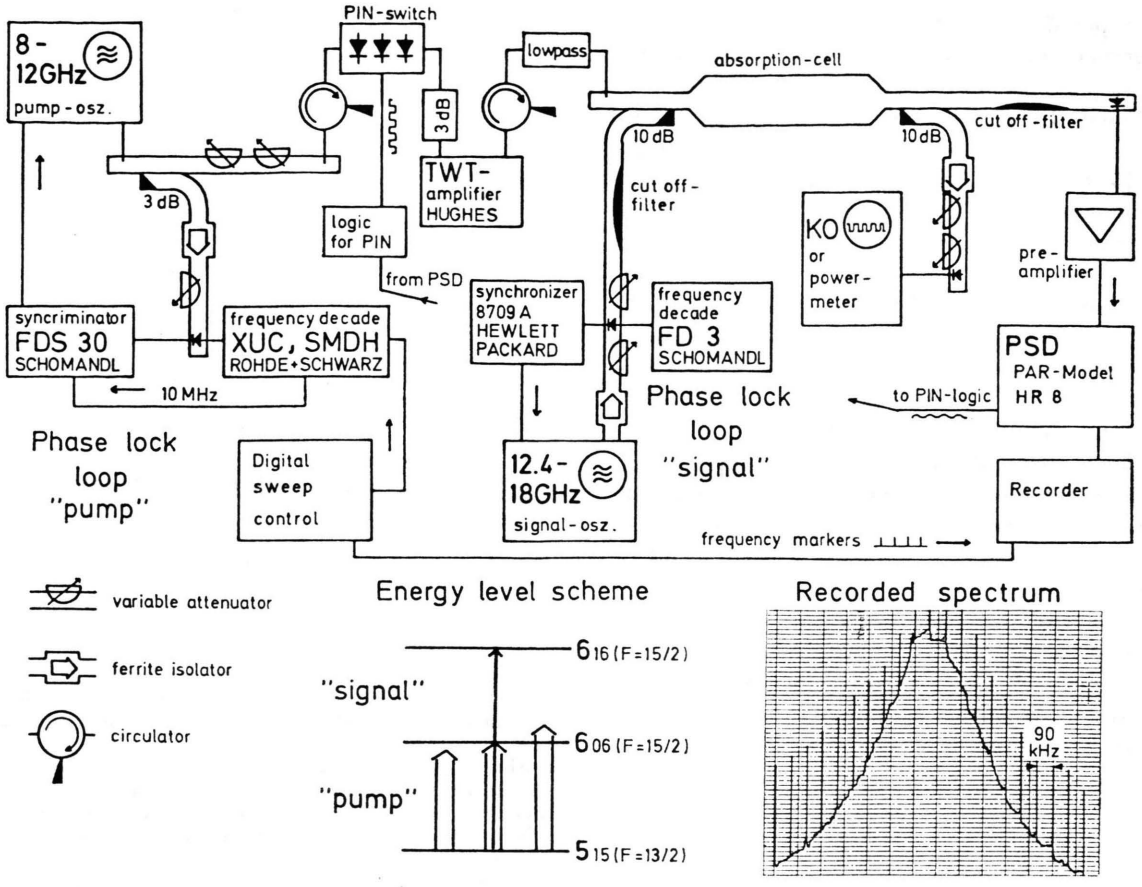

Fig. 4. Microwave-microwave double resonance set up used to confirm the assignment of the μ_a-type spectra and for the localization of the weak μ_b-type transitions of the Bromofuranes. In the latter case the strong pump radiation was slowly swept over the frequency range of the μ_b-type transition (see insert), while the signal frequency was fixed at a well known μ_a-type transition. Only when the pump frequency coincides with the μ_b-type transition a change of signal intensity in phase with the periodically applied pump radiation is observed. For more information the reader is refered to Reference [7].

coupling of one nucleus as given in (1) [8]

$$\hat{H}_{\text{eff}}/h = A\hat{J}_a^2 + B\hat{J}_b^2 + C\hat{J}_c^2 + \tfrac{1}{6}\sum_i\sum_j \hat{Q}_{ij}\hat{V}_{ij}/h\,, \qquad (1)$$

A, B, C rotational constants,

$\hat{J}_a, \hat{J}_b, \hat{J}_c$ operators corresponding to the components of the rotational angular momentum in direction of the principal inertia axes measured in units of $\hbar$,

Q_{ij} components of the Br nuclear quadrupole moment tensor,

$-V_{ij}$ components of the intra molecular electric field gradient tensor at the position of the Br-nucleus.

Equation (1) represents an effective rotational Hamiltonian. It results from a second order perturbation treatment within the rovibronic states which aimes at the vibronic ground state.

A computer program was written in which the corresponding Hamiltonian matrix is set up with respect to the coupled symmetric top basis $|J, K, I, F, M_F\rangle$ [9]. This matrix factorizes into F blocks (F = quantum number corresponding to the overall angular momentum including the spin of the Bromine nucleus (I) and the rotational angular momentum (J), but neglecting all other spins). In the case of the Br-nuclei with nuclear spin $I = 3/2$, each F-block comprises four J blocks and is diagonalized numerically. The good fit of the observed spectra indicates that the effective Hamiltonian given in Eq. (1) provides an excellent approximation for the low J states of the Bromofuranes observed here.

Table 1. Observed and calculated microwave transition frequencies of 2-Bromofurane (79). The calculated frequencies correspond to the molecular parameters listet in Table 5 and were obtained from a complete diagonalization of the effective Hamiltonian (Eq. (1) and Ref. [9]). For comparison we also list the frequencies calculated by the standard 1-st order perturbation treatment i.e. neglecting all matrixelements which are off-diagonal in J. As is seen from the comparison these off-diagonal elements account for line shifts on the order of several hundred kHz and must be clearly included. All frequencies are given in MHz.

Transition								1st order perturbation treatment		Complete diagonalization	
J	K^-	K^+	$\leftarrow J$	K^-	K^+	$F - F$	Freq. obs.	freq. calc.	obs.-calc.	freq. calc.	obs.-calc.
4	2	2	3	2	1	11/2 — 9/2	10083.85	10083.51	0.34	10083.92	— 0.07
						9/2 — 7/2	10142.32	10142.87	— 0.55	10142.35	— 0.03
						7/2 — 5/2	10122.63	10122.07	0.56	10122.68	— 0.05
						5/2 — 3/2	10061.58	10062.72	— 1.14	10061.67	— 0.09
4	0	4	3	0	3	11/2 — 9/2[a]					
						9/2 — 7/2[a]	10047.83	10047.56	0.27	10047.83	0.00
						7/2 — 5/2	10064.32	10064.70	— 0.38	10064.28	0.04
						5/2 — 3/2	10065.29	10064.81	0.48	10065.26	0.03
4	1	3	3	1	2	11/2 — 9/2	10408.48	10408.11	0.37	10408.44	0.04
						9/2 — 7/2	10422.76	10422.89	— 0.13	10422.71	0.05
						7/2 — 5/2	10430.77	10430.76	0.01	10430.75	0.02
						5/2 — 3/2	10415.44	10415.97	— 0.53	10415.43	0.01
4	1	4	3	1	3	11/2 — 9/2	9722.95	9722.65	0.30	9722.92	0.03
						9/2 — 7/2	9737.23	9737.35	— 0.12	9737.18	0.05
						7/2 — 5/2	9744.78	9744.98	— 0.20	9744.74	0.04
						5/2 — 3/2	9729.55	9730.19	— 0.64	9729.52	0.03
4	1	3	4	0	4	11/2 — 11/2[b]	8870.21	8870.47	— 0.26	8870.31	— 0.10
						9/2 — 9/2[b]	8849.94	8849.83	0.11	8850.03	— 0.09
5	2	3	4	2	2	13/2 — 11/2	12636.01	12635.81	0.20	12636.03	— 0.02
						11/2 — 9/2	12665.15	12665.56	— 0.41	12665.15	0.00
						9/2 — 7/2	12661.50	12661.25	0.25	12661.50	— 0.00
						7/2 — 5/2	12630.88	12631.50	— 0.62	12630.89	— 0.01
5	0	5	4	0	4	13/2 — 11/2	12541.57	12541.44	0.13	12541.56	0.01
						11/2 — 9/2	12541.40	12541.30	0.10	12541.32	0.09
						9/2 — 7/2	12551.23	12551.49	— 0.26	12551.18	0.05
						7/2 — 5/2	12551.48	12551.62	— 0.14	12551.44	0.04
5	1	4	4	1	3	13/2 — 11/2	13010.45	13010.24	0.21	13010.43	0.02
						11/2 — 9/2	13017.60	13017.61	— 0.01	13017.55	0.05
						9/2 — 7/2	13024.62	13024.26	0.36	13024.67	— 0.05
						7/2 — 5/2	13016.36	13016.89	— 0.53	13016.29	0.07
5	1	5	4	1	4	13/2 — 11/2	12153.93	12153.74	0.19	12153.91	0.02
						11/2 — 9/2	12161.02	12161.12	— 0.10	12161.03	— 0.01
						9/2 — 7/2	12167.44	12167.58	— 0.14	12167.41	0.03
						7/2 — 5/2	12159.87	12160.20	— 0.33	12159.89	— 0.02
5	2	4	4	2	3	13/2 — 11/2	12581.09	12580.79	0.30	12581.07	0.02
						11/2 — 9/2	12610.11	12610.40	— 0.28	12610.07	0.04
						9/2 — 7/2	12606.37	12606.11	0.26	12606.37	0.00
5	1	4	5	0	5	13/2 — 13/2[c]	9339.20	9339.27	— 0.07	9339.17	0.03
						11/2 — 11/2[c]	9326.40	9326.14	0.26	9326.26	0.14
						9/2 — 9/2[c]	9329.96	9329.84	0.12	9329.99	— 0.03
						7/2 — 7/2[c]	9342.76	9342.97	— 0.21	9342.67	0.09
6	2	4	5	2	3	15/2 — 13/2	15194.98	15194.80	0.18	15195.05	— 0.07
						13/2 — 11/2	15211.78	15211.87	— 0.09	15211.77	0.01
						11/2 — 9/2	15212.02	15211.91	0.10	15212.03	— 0.01
						9/2 — 7/2	15194.46	15194.85	— 0.39	15194.52	— 0.06

Table 1. continued.

Transition								1st order perturbation treatment		Complete diagonalization	
J	K^-	K^+	← J	K^-	K^+	$F - F$	Freq. obs.	freq. calc.	obs.-calc.	freq. calc.	obs.-calc.
6	0	6	5	0	5	15/2 — 13/2[d]	15021.40	15021.29	0.11	15021.38	0.02
						13/2 — 11/2[d]	15021.25	15021.13	0.12	15021.17	0.08
						11/2 — 9/2[d]	15027.83	15027.92	— 0.09	15027.74	0.09
						9/2 — 7/2[d]	15028.00	15028.08	— 0.08	15027.99	0.01
6	1	5	5	1	4	15/2 — 13/2	15607.25	15607.11	0.14	15607.23	0.02
						13/2 — 11/2	15611.29	15611.30	— 0.01	15611.28	0.01
						11/2 — 9/2	15616.02	15616.46	— 0.44	15615.93	0.09
						9/2 — 7/2	15612.43	15612.27	0.16	15612.49	— 0.06
6	1	6	5	1	5	15/2 — 13/2	14580.29	14580.14	0.15	14580.25	0.04
						13/2 — 11/2	14584.33	14584.34	— 0.01	14584.31	0.02
						11/2 — 9/2	14589.29	14589.45	— 0.16	14589.29	0.00
						9/2 — 7/2	14585.02	14585.17	— 0.15	14585.03	— 0.01
6	2	5	5	2	4	15/2 — 13/2	15099.05	15098.91	0.14	15099.09	— 0.04
						13/2 — 11/2	15115.72	15115.81	— 0.09	15115.64	0.08
						11/2 — 9/2	15115.91	15115.88	0.03	15115.99	— 0.08
						9/2 — 7/2	15098.71	15098.97	— 0.26	15098.65	0.06
6	1	5	6	0	6	15/2 — 15/2[e]	9925.04	9925.08	— 0.04	9925.02	0.02
						13/2 — 13/2[e]	9916.34	9916.30	0.04	9916.38	— 0.04
						11/2 — 11/2[e]	9918.18	9918.38	— 0.20	9918.18	0.00
						9/2 — 9/2[e]	9927.20	9927.16	0.04	9927.18	0.02
6	0	6	5	1	5	15/2 — 13/2[f]	8251.77	8251.60	0.17	8251.76	0.01
						13/2 — 11/2[f]	8267.18	8267.32	— 0.14	8267.19	— 0.01
						11/2 — 9/2[f]	8269.61	8269.63	— 0.02	8269.60	0.01
						9/2 — 7/2[f]	8253.56	8253.91	— 0.35	8253.62	— 0.06
7	2	5	6	2	4	17/2 — 15/2	17764.84	17764.71	0.14	17764.91	— 0.06
						15/2 — 13/2	17775.33	17775.44	— 0.11	17775.36	— 0.03
						13/2 — 11/2	17776.80	17776.73	0.07	17776.85	— 0.05
						11/2 — 9/2	17765.75	17766.00	— 0.25	17765.81	— 0.05
7	0	7	6	0	6	17/2 — 15/2[g]	17485.28	17485.22	0.06	17485.29	— 0.01
						15/2 — 13/2[g]	17485.06	17485.04	0.02	17485.07	— 0.01
						13/2 — 11/2[g]	17489.89	17489.91	— 0.02	17489.86	0.03
						11/2 — 9/2[g]	17490.13	17490.09	0.04	17490.11	0.02
7	1	6	6	1	5	17/2 — 15/2	18198.71	18198.62	0.09	18198.71	0.00
						15/2 — 13/2	18201.21	18201.21	0.00	18201.21	0.00
						13/2 — 11/2	18205.15	18205.23	— 0.08	18205.17	— 0.02
						11/2 — 9/2	18202.52	18202.64	— 0.12	18202.54	— 0.02
7	1	7	6	1	6	17/2 — 15/2	17002.24	17002.16	0.08	17002.24	0.00
						15/2 — 13/2	17004.79	17004.76	0.03	17004.76	0.03
						13/2 — 11/2	17008.59	17008.38	0.21	17008.59	0.00
						11/2 — 9/2	17005.97	17706.09	— 0.12	17005.97	0.00
7	0	7	6	1	6	17/2 — 15/2[h]	11156.80	11156.68	0.12	11156.80	0.00
						15/2 — 13/2[h]	11168.01	11168.03	— 0.02	11167.96	0.05
						13/2 — 11/2[h]	11170.18	11170.17	0.01	11170.17	0.01
						11/2 — 9/2[h]	11158.71	11158.83	— 0.12	11158.70	0.01

[a] Intensity weighted mean.
Transitions measured using mw-mw double resonance:
[b] Pump on 4 1 3 — 4 0 4, signal on 5 1 4 — 4 1 3.
[c] Pump on 5 1 4 — 5 0 5, signal on 6 1 5 — 5 1 4.
[d] Pump on 5 1 4 — 5 0 5, signal on 6 0 6 — 5 0 5.
[e] Pump on 6 1 5 — 6 0 6, signal on 6 1 5 — 5 1 4.
[f] Pump on 6 0 6 — 5 1 5, signal on 6 1 6 — 5 1 5.
[g] Pump on 7 0 7 — 6 1 6, signal on 7 0 7 — 6 0 6.
[h] Pump on 7 0 7 — 6 1 6, signal on 7 1 7 — 6 1 6.

Table 2. Observed and calculated microwave transition frequencies of 2-Bromofurane (81) calculated from the molecular parameters listed in Table 5.

Transition								1st order perturbation treatment		Complete diagonalization	
J	K^-	K^+	$\leftarrow J$	K^-	K^+	$F - F$	Freq. obs.	freq. calc.	obs.-calc.	freq. calc.	obs.-calc.
4	2	2	3	2	1	11/2 — 9/2	9992.48	9992.30	0.18	9992.57	— 0.09
						9/2 — 7/2	10041.51	10041.89	— 0.38	10041.55	— 0.04
						7/2 — 5/2	10024.86	10024.51	0.35	10024.95	— 0.09
						5/2 — 3/2	9974.06	9974.92	— 0.86	9974.15	— 0.09
4	0	4	3	0	3	11/2 — 9/2[a]	9955.72	9955.53	0.19	9955.70	0.02
						9/2 — 7/2[a]					
						7/2 — 5/2	9969.59	9969.86	— 0.27	9969.55	0.04
						5/2 — 3/2	9970.20	9969.95	0.25	9970.22	— 0.02
4	1	3	3	1	2	11/2 — 9/2	10309.86	10309.65	0.21	10309.87	— 0.01
						9/2 — 7/2	10321.89	10322.00	— 0.12	10321.88	0.01
						7/2 — 5/2	10328.53	10328.58	— 0.04	10328.57	— 0.04
						5/2 — 3/2	10315.79	10316.22	— 0.43	10315.83	— 0.05
4	1	4	3	1	3	11/2 — 9/2	9636.99	9636.79	0.20	9636.97	0.02
						9/2 — 7/2	9648.99	9649.15	— 0.16	9648.97	0.02
						7/2 — 5/2	9655.33	9655.45	— 0.12	9655.29	0.04
						5/2 — 3/2	9642.67	9643.09	— 0.42	9642.62	0.05
5	2	3	4	2	2	13/2 — 11/2	12518.81	12518.80	0.01	12518.86	— 0.05
						11/2 — 9/2	12544.20	12543.65	0.55	12544.22	— 0.02
						9/2 — 7/2	12540.22	12540.05	0.17	12540.23	— 0.01
						7/2 — 5/2	12514.69	12515.19	— 0.51	12514.75	— 0.06
5	0	5	4	0	4	13/2 — 11/2	12426.83	12426.76	0.07	12426.84	— 0.01
						11/2 — 9/2	12426.69	12426.65	0.04	12426.66	0.03
						9/2 — 7/2	12434.95	12435.16	— 0.22	12434.95	— 0.00
						7/2 — 5/2	12435.19	12435.27	— 0.08	12435.15	0.04
5	1	4	4	1	3	13/2 — 11/2	12886.60	12886.47	0.13	12886.60	0.01
						11/2 — 9/2	12892.60	12892.63	— 0.03	12892.59	0.01
						9/2 — 7/2	12898.05	12898.19	— 0.14	12898.03	0.01
						7/2 — 5/2	12891.83	12892.03	— 0.20	12891.81	0.02
5	1	5	4	1	4	13/2 — 11/2	12045.84	12045.71	0.13	12045.83	0.02
						11/2 — 9/2	12051.85	12051.88	— 0.03	12051.81	0.04
						9/2 — 7/2	12057.17	12057.28	— 0.11	12057.16	0.01
						7/2 — 5/2	12050.91	12051.11	— 0.20	12050.89	0.02
5	2	4	4	2	3	13/2 — 11/2	12466.06	12465.84	0.21	12466.03	0.03
						11/2 — 9/2	12490.38	12490.58	— 0.21	12490.36	0.02
						9/2 — 7/2	12487.22	12487.00	0.22	12487.19	0.03
						7/2 — 5/2	12461.83	12462.26	— 0.43	12461.82	0.01
5	1	4	5	0	5	13/2 — 13/2[b]	9323.58	9323.64	— 0.06	9323.57	0.01
						11/2 — 11/2[b]	9312.82	9312.67	0.15	9312.76	0.06
						9/2 — 9/2[b]	9315.44	9315.77	— 0.33	9315.43	0.01
						7/2 — 7/2[b]	9326.83	9326.73	0.10	9326.74	0.09
6	2	4	5	2	3	15/2 — 13/2	15052.54	15052.31	0.23	15052.55	— 0.01
						13/2 — 11/2	15065.60	15066.57	— 0.97	15065.64	— 0.04
						11/2 — 9/2	15066.66	15066.60	0.05	15066.69	— 0.03
						9/2 — 7/2	15052.10	15052.35	— 0.25	15052.11	— 0.01
6	0	6	5	0	5	15/2 — 13/2[c]	14884.61	14884.56	0.06	14884.61	— 0.00
						13/2 — 11/2[c]	14884.49	14884.43	0.07	14884.45	0.05
						11/2 — 9/2[c]	14890.05	14890.10	— 0.05	14889.97	0.08
						9/2 — 7/2[c]	14890.19	14890.23	— 0.04	14890.16	0.03
6	1	5	5	1	4	15/2 — 13/2	15458.48	15458.43	0.05	15458.51	— 0.03
						13/2 — 11/2	15461.94	15461.93	0.01	15461.92	0.02
						11/2 — 9/2	15466.30	15466.24	0.06	15466.31	— 0.01
						9/2 — 7/2	15462.70	15462.74	— 0.04	15462.69	0.02

Table 2. continued.

Transition								1st order perturbation treatment		Complete diagonalization	
J	K^-	$K^+ \leftarrow J$		K^-	K^+	$F - F$	Freq. obs.	freq. calc.	obs.-calc.	freq. calc.	obs.-calc.
6	1	6	5	1	5	15/2 — 13/2[d]	14450.40	14450.31	0.09	14450.38	0.02
						13/2 — 11/2[d]	14453.82	14453.81	0.00	14453.79	0.03
						11/2 — 9/2[d]	14457.98	14458.02	— 0.04	14457.96	0.02
						9/2 — 7/2[d]	14454.42	14454.51	— 0.10	14454.41	0.01
6	2	5	5	2	4	15/2 — 13/2	14960.11	14960.01	0.10	14960.13	— 0.02
						13/2 — 11/2	14974.02	14974.14	— 0.12	14974.02	0.00
						11/2 — 9/2	14974.26	14974.19	0.07	14974.27	— 0.01
						9/2 — 7/2	14959.81	14960.06	— 0.25	14959.83	— 0.02
6	1	5	6	0	6	15/2 — 15/2[e]	9897.43	9897.51	— 0.08	9897.47	— 0.03
						13/2 — 13/2[e]	9890.21	9890.18	0.03	9890.23	— 0.03
						11/2 — 11/2[e]	9891.83	9891.91	— 0.08	9891.77	0.06
						9/2 — 9/2[e]	9899.35	9899.24	0.10	9899.26	0.09
6	0	6	5	1	5	15/2 — 13/2[d]	8083.55	8083.36	0.20	8083.47	0.09
						13/2 — 11/2[d]	8096.49	8096.52	— 0.03	8096.43	0.06
						11/2 — 9/2[d]	8098.44	8098.44	0.00	8098.42	0.02
						9/2 — 7/2[d]	8085.07	8085.28	— 0.22	8085.07	— 0.00
7	2	5	6	2	4	17/2 — 15/2	17596.68	17596.60	0.08	17596.72	— 0.04
						15/2 — 13/2	17605.45	17605.57	— 0.12	17605.51	— 0.06
						13/2 — 11/2	17606.63	17606.65	— 0.02	17606.72	— 0.08
						11/2 — 9/2	17597.47	17597.68	— 0.21	17597.54	— 0.07
7	0	7	6	0	6	17/2 — 15/2[f]	17327.09	17327.03	0.06	17327.07	0.01
						15/2 — 13/2[f]	17326.91	17326.88	0.03	17326.90	0.01
						13/2 — 11/2[f]	17331.01	17330.95	0.06	17330.99	0.02
						11/2 — 9/2[f]	17330.25	17331.10	— 0.85	17330.25	— 0.00
7	1	7	6	1	6	17/2 — 15/2	16850.83	16850.77	0.07	16850.82	0.01
						15/2 — 13/2	16852.89	16852.94	— 0.05	16852.94	— 0.05
						13/2 — 11/2	16856.16	16856.22	— 0.07	16856.15	0.00
						11/2 — 9/2	16853.98	16854.05	— 0.07	16853.96	0.02
7	0	7	6	1	6	17/2 — 15/2[g]	10960.10	10960.08	0.02	10960.16	— 0.06
						15/2 — 13/2[g]	10969.47	10969.58	— 0.11	10969.54	— 0.07
						13/2 — 11/2[g]	10971.50	10971.37	0.13	10971.45	0.05
						11/2 — 9/2[g]	10960.93	10960.87	0.06	10960.92	0.02
8	1	8	7	1	7	19/2 — 17/2	19247.00	19246.97	0.03	19247.01	— 0.01
						17/2 — 15/2	19248.39	19248.40	— 0.01	19248.41	— 0.02
						15/2 — 13/2	19250.94	19251.01	— 0.07	19250.96	— 0.02
						13/2 — 11/2	19249.48	19249.57	— 0.09	19249.52	— 0.04

[a] Intensity weighted mean.
Transitions measured using mw-mw-double resonance:
[b] Pump on 5 1 4 — 5 0 5, signal on 5 1 4 — 4 1 3.
[c] Pump on 5 1 4 — 5 0 5, signal on 6 0 6 — 5 0 5.
[d] Pump on 6 0 6 — 5 1 5, signal on 6 1 6 — 5 1 5.
[e] Pump on 6 1 5 — 6 0 6, signal on 6 1 5 — 5 1 4.
[f] Pump on 7 0 7 — 6 1 6, signal on 7 0 7 — 6 0 6.
[g] Pump on 7 0 7 — 6 1 6, signal on 7 1 7 — 6 1 6.

Discussion

From the small value of the inertia defects $\Delta I = I_{cc} - (I_{aa} + I_{bb})$ there is no doubt that the equilibrium configurations are indeed planar as expected. (For a rigid planar point mass model the inertia defect would be exactly zero. The small deviations arise from zero point vibrations and, to a lesser extent, from electronic contributions. For a detailled discussion of inertia defects in planar molecules see Ref. [10]). Due to the planarity condition the rotational constants of each isotopic species correspond to only two equations of condition for the structural parameters. With 15 structural parameters to be determined it is clearly impossible to present a conclusive structure at the present stage of our knowledge. Exemplarily however for 3-Bromofurane we tried to optimize four structural param-

eters with respect to the measured rotational constants. Quite arbitrarily we chose the three CC-distances and the C-C-Br-bond angle as variables. All other parameters of the Carbon/Hydrogen frame were fixed to their values in Furane. The C-Br-bond distance was fixed to 1.85 Å, its value in Bromobenzene, and the Oxygen was assumed to sit at the apex of an isosceles triangle with the CO bond distances fixed to their values in Furane. The result of this optimization is shown in Figure 5. The fit is obviously good. However it indicates only that the frame of the Furane ring is probably slightly widened upon Bromine substitution. The detailed numbers of the bond distances should by no means taken too seriously because of the restrictions imposed on the optimization procedure.

We now turn to the discussion of the Bromine quadrupole coupling tensors. In all cases the diagonal elements as well as the absolute value of the only nonvanishing off-diagonal element, χ_{ab}, could be determined from the experiment. In the case of 2-Bromofurane however we are rather confident to know also the sign of χ_{ab} (negative). The argument is as follows. From the initial structure (see also Fig. 6) the C-Br bond intersects the a-axis at an angle of roughly $-4°$. (The C-Br bond points into the quadrant characterized by positive a-values and negative b-values). Essentially the same angle ($-3.9°$ for the ^{79}Br-species and $-3.4°$ for the ^{81}Br-species) is obtained from the diagonalization of the χ-tensor if χ_{ab} is assumed to be negative. This could fit nicely into the picture of a coupling tensor with

Table 3. Observed and calculated microwave transition frequencies of 3-Bromofurane (79) calculated from the molecular parameters listed in column 1 of Table 6.

Transition								1st order perturbation treatment		Complete diagonalization	
J	K^-	$K^+ \leftarrow J'$		K'^-	K'^+	$F - F$	Freq. obs.	freq. calc.	obs.-calc.	freq. calc.	obs.-calc.
4	2	2	3	2	1	11/2 — 9/2	9533.65	9533.28	0.37	9533.69	— 0.05
						9/2 — 7/2	9591.73	9592.25	— 0.52	9591.73	0.01
						7/2 — 5/2	9572.14	9571.58	0.56	9572.23	— 0.09
4	0	4	3	0	3	11/2 — 9/2	9509.22	9509.01	0.21	9509.19	0.03
						9/2 — 7/2	9509.04	9508.94	0.10	9509.05	— 0.01
						7/2 — 5/2	9525.52	9526.04	— 0.52	9525.50	0.02
						5/2 — 3/2	9526.12	9526.12	0.00	9526.16	— 0.04
4	1	3	3	1	2	11/2 — 9/2	9827.08	9826.74	0.34	9827.04	0.04
						9/2 — 7/2	9841.28	9841.44	— 0.16	9841.24	0.04
						7/2 — 5/2	9849.13	9849.21	— 0.08	9849.13	— 0.00
						5/2 — 3/2	9833.94	9834.50	— 0.56	9833.92	0.02
4	1	4	3	1	3	11/2 — 9/2	9217.33	9217.12	0.22	9217.39	— 0.05
						9/2 — 7/2	9231.62	9231.83	— 0.21	9231.56	0.06
						7/2 — 5/2	9239.15	9239.38	— 0.22	9239.15	— 0.00
						5/2 — 3/2	9223.95	9224.66	— 0.71	9223.97	— 0.02
4	2	3	3	2	2	11/2 — 9/2	9512.32	9511.83	0.49	9512.26	0.06
						9/2 — 7/2	9570.33	9570.74	— 0.41	9570.24	0.09
						7/2 — 5/2	9550.77	9550.08	0.69	9550.72	0.05
5	2	3	4	2	2	13/2 — 11/2	11944.40	11944.15	0.24	11944.45	— 0.05
						11/2 — 9/2	11973.35	11973.69	— 0.34	11973.39	— 0.04
						9/2 — 7/2	11969.69	11969.41	0.28	11969.68	0.01
						7/2 — 5/2	11939.24	11939.88	— 0.64	11939.22	0.02
5	0	5	4	0	4	13/2 — 11/2	11872.88	11872.73	0.15	11872.85	0.03
						11/2 — 9/2	11872.72	11872.64	0.08	11872.68	0.03
						9/2 — 7/2	11882.48	11882.76	— 0.28	11882.46	0.02
						7/2 — 5/2	11882.78	11882.85	— 0.06	11882.74	0.05
5	1	5	4	1	4	13/2 — 11/2	11523.07	11522.89	0.18	11523.06	0.01
						11/2 — 9/2	11530.18	11530.24	— 0.05	11530.14	0.04
						9/2 — 7/2	11536.52	11536.69	— 0.16	11536.53	— 0.01
						7/2 — 5/2	11529.06	11529.34	— 0.28	11529.03	0.03

Table 3. continued.

Transition								1st order perturbation treatment		Complete diagonalization	
J	K^-	$K^+ \leftarrow J'$		K'^-	K'^+	$F - F$	Freq. obs.	freq. calc.	obs.-calc.	freq. calc.	obs.-calc.
5	2	4	4	2	3	13/2 — 11/2	11901.59	11901.31	0.28	11901.59	0.01
						11/2 — 9/2	11930.45	11930.76	— 0.31	11930.42	0.03
						9/2 — 7/2	11926.78	11926.49	0.28	11926.77	0.01
						7/2 — 5/2	11896.42	11897.65	— 1.24	11896.40	0.01
5	1	4	5	0	5	13/2 — 11/2[a]	9314.30	9314.31	— 0.01	9314.23	0.07
						11/2 — 9/2[a]	9300.70	9300.73	— 0.03	9300.89	— 0.19
						9/2 — 7/2[a]	9304.00	9304.56	— 0.56	9304.25	— 0.25
						7/2 — 5/2[a]	9318.10	9318.14	— 0.04	9318.27	— 0.17
6	2	4	5	2	3	15/2 — 13/2	14359.48	14359.36	0.13	14359.51	— 0.02
						13/2 — 11/2	14376.08	14376.28	— 0.20	14376.08	— 0.01
						11/2 — 9/2	14376.41	14376.33	0.08	14376.44	— 0.04
						9/2 — 7/2	14359.04	14359.41	— 0.37	14359.05	— 0.02
6	0	6	5	0	5	15/2 — 13/2[b]	14225.50	14225.38	0.12	14225.47	0.04
						13/2 — 11/2[b]	14225.29	14225.27	0.02	14225.31	— 0.03
						11/2 — 9/2[b]	14231.79	14232.01	— 0.22	14231.83	— 0.04
						9/2 — 7/2[b]	14232.02	14232.12	— 0.11	14232.05	— 0.03
6	1	5	5	1	4	15/2 — 13/2	14738.39	14738.27	0.13	14738.38	0.01
						13/2 — 11/2	14742.44	14742.44	— 0.00	14742.43	0.01
						11/2 — 9/2	14747.49	14747.55	— 0.06	14747.48	0.01
						9/2 — 7/2	14743.23	14743.37	— 0.14	14743.23	— 0.00
6	1	6	5	1	5	15/2 — 13/2	13824.79	13824.67	0.12	13824.78	0.01
						13/2 — 11/2	13828.82	13828.85	— 0.03	13828.82	0.01
						11/2 — 9/2	13833.76	13833.87	— 0.11	13833.78	— 0.02
						9/2 — 7/2	13829.52	13829.69	— 0.17	13829.55	— 0.02
6	2	5	5	2	4	15/2 — 13/2	14284.79	14284.62	0.16	14284.80	— 0.02
						13/2 — 11/2	14301.26	14301.44	— 0.18	14301.26	— 0.00
						11/2 — 9/2	14301.60	14301.50	0.10	14301.62	— 0.02
						9/2 — 7/2	14284.31	14284.69	— 0.38	14284.33	— 0.03
6	1	5	6	0	6	15/2 — 13/2[c]	9827.20	9827.20	0.00	9827.14	0.06
						13/2 — 11/2[c]	9818.18	9817.90	0.28	9818.01	0.18
						11/2 — 9/2[c]	9820.08	9820.10	— 0.02	9819.91	0.17
						9/2 — 7/2[c]	9829.54	9829.39	0.15	9829.46	0.08
7	2	5	6	2	4	17/2 — 15/2	16782.86	16782.79	0.07	16782.92	— 0.06
						15/2 — 13/2	16793.29	16793.42	— 0.13	16793.32	— 0.04
						13/2 — 11/2	16794.68	16794.71	— 0.03	16794.75	— 0.07
						11/2 — 9/2	16783.80	16784.08	— 0.28	16783.88	— 0.07
7	0	7	6	0	6	17/2 — 15/2[d]	16565.51	16565.41	0.10	16565.48	0.03
						15/2 — 13/2[d]	16565.34	16565.29	0.06	16565.32	0.02
						13/2 — 11/2[d]	16570.01	16570.12	— 0.12	16569.99	0.02
						11/2 — 9/2[d]	16570.20	16570.25	— 0.04	16570.18	0.03
7	1	7	6	1	6	17/2 — 15/2	16122.90	16122.84	0.07	16122.92	— 0.01
						15/2 — 13/2	16125.42	16125.44	— 0.02	16125.43	— 0.02
						13/2 — 11/2	16129.26	16129.35	— 0.09	16129.25	0.01
						11/2 — 9/2	16126.65	16126.75	— 0.10	16126.61	0.04
7	0	7	6	1	6	17/2 — 15/2[e]	9937.32	9937.27	0.05	9937.39	— 0.07
						15/2 — 13/2[e]	9948.22	9948.31	— 0.09	9948.22	— 0.00
						13/2 — 11/2[e]	9950.45	9950.51	— 0.06	9950.44	0.01
						11/2 — 9/2[e]	9939.18	9939.47	— 0.29	9939.20	— 0.02

Transitions measured using mw-mw double resonance:
[a] Pump on 5 1 4 — 5 0 5, signal on 6 1 5 — 5 1 4.
[b] Pump on 5 1 4 — 5 0 5, signal on 6 0 6 — 5 0 5.
[c] Pump on 6 1 5 — 6 0 6, signal on 6 1 5 — 5 1 4.
[d] Pump on 7 0 7 — 6 1 6, signal on 7 0 7 — 6 0 6.
[e] Pump on 7 0 7 — 6 1 6, signal on 7 1 7 — 6 1 6.

Table 4. Observed and calculated microwave transition frequencies of 3-Bromofurane (81) calculated according to Eq. (1) from the molecular parameters listed in column 2 of Table 6.

Transition								1st order perturbation treatment		Complete diagonalization	
J	K^-	K^+	← J	K^-	K^+	$F - F$	Freq. obs.	freq. calc.	obs.-calc.	freq. calc.	obs.-calc.
4	2	2	3	2	1	11/2 — 9/2	9446.45	9446.21	0.24	9446.46	— 0.01
						9/2 — 7/2	9495.09	9495.51	— 0.42	9495.18	— 0.09
						7/2 — 5/2	9478.65	9478.23	0.42	9478.68	— 0.03
4	0	4	3	0	3	11/2 — 9/2	9420.90	9420.74	0.16	9420.86	0.04
						9/2 — 7/2	9420.75	9420.67	0.08	9420.74	0.01
						7/2 — 5/2	9434.62	9434.97	— 0.35	9434.59	0.03
						5/2 — 3/2	9435.02	9435.03	— 0.01	9435.05	— 0.03
4	1	3	3	1	2	11/2 — 9/2	9733.05	9732.81	0.24	9733.02	0.03
						9/2 — 7/2	9745.03	9745.11	— 0.08	9744.96	0.07
						7/2 — 5/2	9751.53	9751.60	— 0.07	9751.54	— 0.01
						5/2 — 3/2	9738.92	9739.30	— 0.38	9738.90	0.02
4	1	4	3	1	3	11/2 — 9/2	9134.78	9134.57	0.21	9134.76	0.02
						9/2 — 7/2	9146.69	9146.87	— 0.18	9146.68	0.01
						7/2 — 5/2	9152.99	9153.17	— 0.18	9153.00	— 0.01
						5/2 — 3/2	9140.40	9140.87	— 0.47	9140.39	0.01
4	2	3	3	2	2	11/2 — 9/2	9425.93	9425.59	0.34	9425.89	0.04
						9/2 — 7/2	9474.53	9474.82	— 0.29	9474.47	0.06
						7/2 — 5/2	9458.06	9457.56	0.51	9458.01	0.06
5	2	3	4	2	2	13/2 — 11/2	11832.66	11832.48	0.18	11832.73	— 0.07
						11/2 — 9/2	11856.90	11857.17	— 0.27	11856.91	— 0.01
						9/2 — 7/2	11853.77	11853.59	0.17	11853.78	— 0.01
						7/2 — 5/2	11828.44	11828.91	— 0.47	11828.45	— 0.01
5	0	5	4	0	4	13/2 — 11/2	11762.71	11762.59	0.13	11762.67	0.04
						11/2 — 9/2	11762.57	11762.51	0.06	11762.54	0.03
						9/2 — 7/2	11770.79	11770.96	— 0.18	11770.75	0.03
						7/2 — 5/2	11771.01	11771.04	— 0.03	11770.97	0.04
5	1	5	4	1	4	13/2 — 11/2	11419.10	11418.97	0.13	11419.09	0.01
						11/2 — 9/2	11425.06	11425.11	— 0.06	11425.05	0.01
						9/2 — 7/2[a]	11430.45	11430.50	— 0.05	11430.39	0.06
						7/2 — 5/2	11424.20	11424.36	— 0.16	11424.14	0.06
5	2	4	4	2	3	13/2 — 11/2	11791.50	11791.28	0.22	11791.47	0.03
						11/2 — 9/2	11815.68	11815.88	— 0.20	11815.65	0.03
						9/2 — 7/2	11812.55	11812.32	0.22	11812.51	0.04
						7/2 — 5/2	11787.26	11787.71	— 0.45	11787.26	0.01
5	1	4	5	0	5	13/2 — 13/2[b]	9300.80	9300.99	— 0.19	9300.93	— 0.13
						11/2 — 11/2[b]	9289.68	9289.70	— 0.02	9289.82	— 0.14
						9/2 — 9/2[b]	9292.50	9292.89	— 0.39	9292.68	— 0.18
						7/2 — 7/2[b]	9304.07	9304.17	— 0.10	9304.27	— 0.20
6	0	6	5	0	5	15/2 — 13/2[c]	14093.89	14093.85	0.04	14093.92	— 0.03
						13/2 — 11/2[c]	14093.77	14093.76	0.01	14093.79	— 0.02
						11/2 — 9/2[c]	14099.21	14099.40	— 0.18	14099.27	— 0.06
						9/2 — 7/2[c]	14099.40	14099.49	— 0.10	14099.44	— 0.04
6	1	5	5	1	4	15/2 — 13/2	14596.38	14596.28	0.10	14596.36	0.02
						13/2 — 11/2	14599.80	14599.78	0.03	15599.76	0.04
						11/2 — 9/2	14604.00	14604.05	— 0.05	14603.99	0.01
						9/2 — 7/2	14600.47	14600.56	— 0.08	14600.46	0.02
6	1	6	5	1	5	15/2 — 13/2[a]	13699.81	13699.71	0.10	13699.79	0.02
						13/2 — 11/2[a]	13703.20	13703.21	— 0.01	13703.19	0.01
						11/2 — 9/2[a]	13707.32	13707.40	— 0.08	13707.38	— 0.06
						9/2 — 7/2[a]	13703.79	13703.91	— 0.12	13703.76	0.02

Table 4. continued.

Transition								1st order perturbation treatment		Complete diagonalization	
J	K^-	$K^+ \leftarrow J$		K^-	K^+	$F - F$	Freq. obs.	freq. calc.	obs.-calc.	freq. calc.	obs.-calc.
6	2	5	5	2	4	15/2 — 13/2	14151.72	14151.58	0.14	14151.71	0.01
						13/2 — 11/2	14165.52	14165.64	— 0.12	14165.51	0.01
						11/2 — 9/2	14165.73	14165.69	0.04	14165.77	— 0.04
						9/2 — 7/2	14151.44	14151.64	— 0.20	14151.39	0.05
6	1	5	6	0	6	15/2 — 15/2[d]	9803.55	9803.42	0.14	9803.38	0.17
						13/2 — 13/2[d]	9795.92	9795.71	0.21	9795.79	0.13
						11/2 — 11/2[d]	9797.52	9797.53	— 0.01	9797.40	0.12
						9/2 — 9/2[d]	9805.40	9805.23	0.17	9805.28	0.12
7	2	5	6	2	4	17/2 — 15/2	16622.69	16622.65	0.05	16622.74	— 0.04
						15/2 — 13/2	16631.42	16631.53	— 0.11	16631.47	— 0.05
						13/2 — 11/2	16632.59	16632.61	— 0.02	16632.64	— 0.05
						11/2 — 9/2	16623.54	16623.73	— 0.18	16623.58	— 0.04
7	0	7	6	0	6	17/2 — 15/2[e]	16413.08	16413.00	0.08	16413.05	0.03
						15/2 — 13/2[e]	16412.95	16412.90	0.05	16412.92	0.02
						13/2 — 11/2[e]	16416.84	16416.94	— 0.10	16416.85	— 0.00
						11/2 — 9/2[e]	16417.01	16417.05	— 0.04	16417.00	0.01
7	1	7	6	1	6	17/2 — 15/2	15977.14	15977.06	0.07	15977.12	0.02
						15/2 — 13/2	15979.21	15979.24	— 0.03	15979.23	— 0.02
						13/2 — 11/2	15982.42	15982.51	— 0.09	15982.39	0.03
						11/2 — 9/2	15980.23	15980.33	— 0.10	15980.27	— 0.04
7	0	7	6	1	6	17/2 — 15/2[f]	9749.07	9748.99	0.08	9749.07	— 0.00
						15/2 — 13/2[f]	9758.17	9758.29	— 0.12	9758.22	— 0.05
						13/2 — 11/2[f]	9760.04	9760.11	— 0.07	9760.02	0.03
						11/2 — 9/2[f]	9750.60	9750.81	— 0.21	9750.67	— 0.07

Transitions measured using mw-mw double resonance:
[a] Pump on 5 1 5 — 4 1 4, signal on 6 1 6 — 5 1 5.
[b] Pump on 5 1 4 — 5 0 5, signal on 6 1 5 — 5 1 4.
[c] Pump on 5 1 4 — 5 0 5, signal on 6 0 6 — 5 0 5.
[d] Pump on 6 1 5 — 6 0 6, signal on 6 1 5 — 5 1 4.
[e] Pump on 7 0 7 — 6 1 6, signal on 7 0 7 — 6 0 6.
[f] Pump on 7 0 7 — 6 1 6, signal on 7 1 7 — 6 1 6.

Table 5. Rotational constants (MHz), principal moments of inertia (amu Å^2) and nuclear quadrupole coupling constants (MHz) of the two isotopic species of 2-Bromofurane. Only $|\chi_{ab}|$ is determined from the hyperfine splittings, but a positive sign would correspond to an eight degree tilt between the C-Br-bond and the principal axes system of the quadrupole coupling tensor which appears highly unlikely. The experimental uncertainties correspond to one standard deviation of the least squares fit to the frequencies listed in Tables 1 and 2 resp.

	$C_4H_3O^{79}Br$	$C_4H_3O^{81}Br$
A	9231.722 ± 0.012	9231.755 ± 0.011
B	1345.671 ± 0.001	1332.366 ± 0.001
C	1174.243 ± 0.001	1164.095 ± 0.000
$\varkappa$	— 0.957	— 0.958
I_a	54.743 ± 0.002	54.743 ± 0.002
I_b	375.557 ± 0.010	379.307 ± 0.011
I_c	430.385 ± 0.012	434.136 ± 0.012
ΔI	0.084 ± 0.016	0.086 ± 0.016
$\chi_{bb} + \chi_{cc}$	— 592.8 ± 0.3	— 495.5 ± 0.3
$\chi_{bb} - \chi_{cc}$	— 11.1 ± 0.2	— 9.3 ± 0.2
χ_{ab}	— 60.6 ± 1.8	— 44.2 ± 2.5

Table 6. Rotational constants (MHz), principal moments of inertia (amu Å^2) and nuclear quadrupole coupling constants (MHz) of the two isotopic species of 3-Bromofurane. Conversion factor [11]: 505.376 ± 14 MHz amu Å^2 $\chi_{aa} = |e| Q V_{aa}/h$ etc.

	$C_4H_3O^{79}Br$	$C_4H_3O^{81}Br$
A	9297.815 ± 0.022	9297.792 ± 0.020
B	1268.089 ± 0.001	1255.437 ± 0.001
C	1115.641 ± 0.001	1105.837 ± 0.001
$\varkappa$	— 0.963	— 0.963
I_a	54.354 ± 0.002	54.354 ± 0.002
I_b	398.533 ± 0.011	402.550 ± 0.011
I_c	452.992 ± 0.013	457.008 ± 0.013
ΔI	0.105 ± 0.017	0.104 ± 0.017
$\chi_{bb} + \chi_{cc}$	— 589.5 ± 0.4	— 492.3 ± 0.4
$\chi_{bb} - \chi_{cc}$	— 7.6 ± 0.3	— 6.8 ± 0.3
$\lvert\chi_{ab}\rvert$	19.9 ± 6.5	16.7 ± 2.0

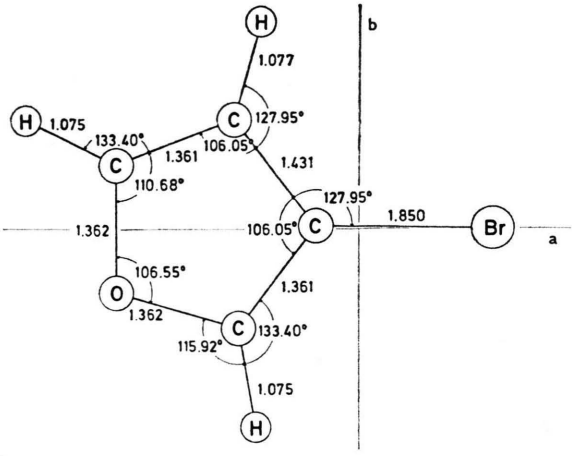

a) Initial structure (undistorted ring)

$^{79}A_{calc} = 9380.116$ $^{81}A_{calc} = 9380.116$
$^{79}B_{calc} = 1273.015$ $^{81}B_{calc} = 1260.329$
$^{79}C_{calc} = 1120.894$ $^{81}C_{calc} = 1111.047$

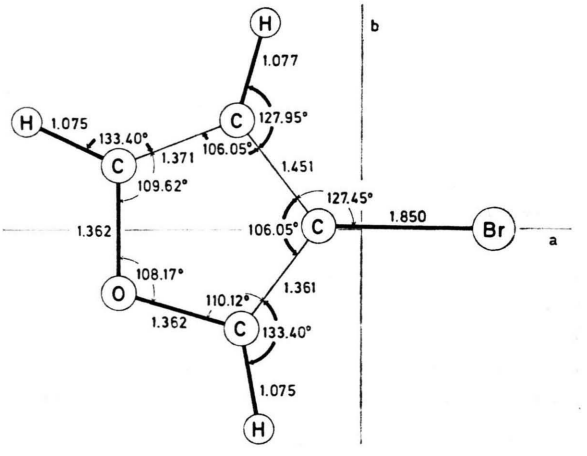

b) Optimized structure

$^{79}A_{calc} = 9297.485$ $^{81}A_{calc} = 9297.484$
$^{79}B_{calc} = 1268.007$ $^{81}B_{calc} = 1255.375$
$^{79}C_{calc} = 1115.828$ $^{81}C_{calc} = 1106.034$

Fig. 5. Initial (a) and optimized (b) structures of 3-Bromofurane and rotational constants calculated for these structures within the rigid rotor model. The superscripts 79 and 81 indicate the bromine isotopic species. In Fig. (b) structural parameters which were kept fixed to their values in the initial structure during the optimization procedure are set off by bold face drawing. Bromine substitution appears to widen the Furane ring slightly. However even though the observed rotational constants are reproduced very well (see Table 6), the individual structural parameters should not be taken too seriously in view of the severe restraints imposed on the optimization procedure.

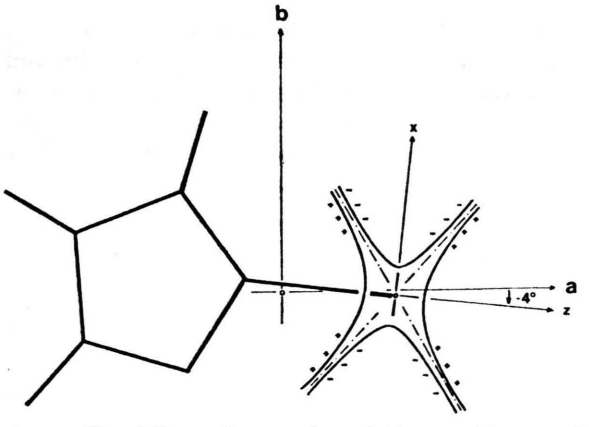

Fig. 6. For 2-Bromofurane the relative positions and orientations of the molecular principal inertia axes system (a, b, c-system) and the principal axes system of the Bromine quadrupole coupling tensor x, y, z-system) are shown schematically in this drawning. It is assumed that the z-axis of the quadrupole coupling tensor is closely aligned to the C-Br-bond. This corresponds to a negative sign of X_{ab}. (Only $|X_{ab}|$ is determined from the hyperfine splittings). If X_{ab} were positive, the angle between the a- and z-axes would be positive. This would correspond to an eight degree tilt angle between the bond and the z-axis of the quadrupole tensor. Since the quadrupole coupling tensor is caused mainly by the charge distribution in the immediate surrounding of the nucleus which is perturbed principally by bonding and very little by the distant charges, such a large tilt angle appears highly unlikely.

its axis essentially aligned to the C-Br bond. The opposite sign of χ_{ab} would correspond to an eight degree tilt between the χ-tensor axis and the C-Br bond which appears highly unlikely. For the 3-Bromofuranes this type of argument fails since here the C-Br bond almost parallels the a-axis. Thus the present uncertainties in the structure could flip the small negative a/C-Br angle to a small positive value with the corresponding change in the sign proposed for χ_{ab}.

The remaining uncertainty as to the sign of χ_{ab} is not serious as far as the estimate of the π-character in the C-Br bond is concerned. This estimate is based on the difference of the in-plane minus the out-of-plane quadrupole coupling tensor elements in its own principal axes system and this difference depends only on the square of χ_{ab}. The degree of π-bonding is usually calculated from Ex. (2) [11, 12].

$$\delta = \frac{2}{3}\frac{\chi_{xx} - \chi_{yy}}{|e|\,Q\,q_{n10}}h\,. \qquad (2)$$

In (2) $|e|\,Q$ is the nuclear quadrupole moment and q_{n10} is the atomic expectation value for the second derivative of the intramolecular Coulomb potential which would be caused by an electron in the valence

shell p_z-orbital of the Bromine atom:

$$q_{n10} = -|e|\left\langle p_z \left| \frac{3z^2}{r^5} - \frac{1}{r^3} \right| p_z \right\rangle. \quad (3)$$

For the orientation of the x, y, z-coordinate system see Figure 6.

Within a simplified valence shell LCAO molecular orbital treatment, in which all nuclear contributions to the field gradient are neglected as well as electronic contributions associated with atomic wavefunctions centred on the other nuclei, δ is equal to the population difference of the in plane and out of plane p-orbitals perpendicular to the sigma bond:

$$\delta = P_{p_x p_x} - P_{p_y p_y}. \quad (4)$$

In (4) the populations are defined as the corresponding elements of the density matrix, i.e.

$$P_{p_x p_x} = 2 \sum_{m}^{\text{occ. orb.}} |C_{m p_x}|^2$$

with $C_{m p_x}$ the coefficient of the Bromine p_x wavefunction in the m-th molecular orbital. Under the assumption that the in-plane p-population perpendicular to the C-Br bond, $P_{p_x p_x}$, is 2 (uneffected by the bond formation), δ corresponds to the shift of atomic electrons into the molecular π-system.

With $(|e|\, Qq_{n10})/h$ values from the work of King and Jaccerino [13] (−769.756 MHz for ^{79}Br and −643.033 MHz for ^{81}Br) the δ-values listed in Table 7 are obtained. Also listed for comparison are the δ-values of some related molecules. With δ-values corresponding to π-contributions on the order of only 1% one probably approaches the limit of the MO model used for the interpretation of the $\chi_{xx} - \chi_{yy}$ difference. The values indicate however that in the less aromatic Furanes π-contributions to the C-X bond are smaller than in the corresponding Halobenzenes.

Table 7. Population differences between the out off plane and in plane Bromine-p-populations perpendicular to the CBr-bond calculated from the measured quadrupole coupling constants according to Eq. (2) of the text. With δ-values corresponding to π-contributions of only 1% or less for the Furanes and Thiophenes one probably approaches the limit of the MO-model used for the interpretation of the $\chi_{xx} - \chi_{yy}$ difference. (For the orientation of the coordinate system see Figure 6).

2-Bromofurane[a]	0.013
3-Bromofurane[a]	0.007
2-Bromothiophene[b]	0.004
2-Chlorothiophene[c]	0.006
Chlorobenzene[c]	0.033
Bromobenzene[c]	0.023
Iodobenzene[d]	0.018

[a] This work.
[b] P. J. Mjöberg, W. M. Ralowski, and S. O. Ljunggren, Z. Naturforsch. **30a**, 541 (1975).
[c] W. Caminati and A. M. Mirri, Chem. Phys. Lett. **12**, 127 (1971).
[d] A. M. Mirri and W. Caminati, Chem. Phys. Lett. **8**, 409 (1971).

We wish to thank Prof. H. Dreizler and Prof. A. Guarnieri for critically reading the manuscript and Prof. A. Bauder for a test run of the Zürich quadrupole hfs program (see ref. 9) against our program. This work was supported by Deutsche Forschungsgemeinschaft and Fonds der Chemie.

The numerical calculations were carried out at the Computer Center of the University of Kiel.

[1] A. F. Shepard, N. R. Winslow, and J. R. Johnson, J. Amer. Chem. Soc. **52**, 2083 (1930).
[2] R. H. Hughes and E. Bright Wilson Jr., Phys. Rev. **71**, 562L (1947).
[3] M. H. Sirvetz, J. Chem. Phys. **19**, 1609L (1951).
[4] Handbook of Chem. and Phys. 56th Ed. (1975). The Chemical Rubber Co., Cleveland Ohio.
[5] P. Nösberger, A. Bauder, and Hs. H. Günthard, Chem. Phys. **1**, 418 (1973).
[6] E. Rosenthal and B. P. Dailey, J. Chem. Phys. **43**, 2093 (1965).
[7] G. K. Pandey and H. Dreizler, Z. Naturforsch. **31a**, 357 (1976).
[8] C. H. Townes and A. L. Schawlow, Microwave spectroscopy, McGrawHill Book Company, New York 1955, Chapts. 5.7 and 6.
[9] For a derivation and a listing of the matrix elements see H. P. Benz, A. Bauder, and Hs. H. Günthard, J. Mol. Spectr. **21**, 156 (1966).
[10] T. Oka and Y. Morino, J. Mol. Spectry. **6**, 472 (1961).
[11] Walter Gordy and Robert L. Cook, Microwave molecular spectra, Vol. IX, Part II of the series Technique of Organic Chemistry, A. Weissberger editor, Interscience Publishers, New York 1970.
[12] J. H. Goldstein, J. Chem. Phys. **24**, 106 (1955).
[13] J. G. King and V. Jaccerino, Phys. Rev. **94**, 1610 (1954).